Pion correlation from Skyrmion-antiSkyrmion annihilation

Yang Lu and R. D. Amado

Department of Physics,

University of Pennsylvania, Philadelphia, PA 19104, USA

(July 13, 1995)

Abstract

We study two pion correlations from Skyrmion and antiSkyrmion collision, using the product ansatz and an approximate random grooming method for nucleon projection. The spatial-isospin coupling inherent in the Skyrme model, along with empirical averages, leads to correlations not only among pions of like charges but also among unlike charge types.

Typeset using REVTEX

I. INTRODUCTION

We have studied nucleon–antinucleon annihilation at rest in the large N_c limit of QCD in a series of papers [1–3]. The gross features of annihilation emerge correctly from this picture. These features include the pion momentum distribution, number and charge spectra and branching ratios into meson channels. In these studies the initial baryon density distribution was taken as spherically symmetric and only the subsequent evolution of the mesons was treated dynamically. In the large N_c limit this dynamics is the classical dynamics of Skyrme like models. To discuss annihilation in flight, pion correlations, the effects of the spin and isospin of the individual baryons and the initial state dynamics involves considerable improvement and sophistication of our previous starting point. We also need to address the question of quantum, or finite N_C, corrections. These are usually introduced by rotating the Hedgehog (and antiHedgehog) slowly and quantizing the rotational degrees of freedom. In the Skyrme picture of $\overline{N}N$ collision, we need to collide a rotating Skyrmion with a rotating antiSkyrmion, project out the nucleon and antinucleon states, and follow the dynamical evolution of the classical system to pion radiation. This is, of course, a much more demanding task than the study of classical dynamics of annihilation without grooming [4], which is already an elaborate and numerically challenging calculation. These difficult issues of classical Skyrmion dynamics and quantum correction in annihilation bear strongly on pion Bose-Einstein correlations [5], charge asymmetry [6,7] in $\overline{p}p \to \pi^+\pi^-$ and annihilation in flight in general.

This paper is a first modest step in the study of annihilation in flight and of pion intensity correlations. We study annihilation in flight with the product ansatz and with no subsequent pion dynamics. Pion intensity correlations emerge as a consequence of random grooming of approaching Skyrmion and antiSkyrmion. The result are similar to the commonly considered Bose-Einstein effects resulting from thermal decoherence. However, the correlation in the present study results from the spatial-isospin coupling inherent in Skyrme soliton. Pion correlations from this spatial-isospin coupling were studied by Blaizot and Diakonov [8] in

2

heavy ion collision.

In the next section, we obtain slowly moving Skyrmion configurations from Galilean transformation. We approximate the full dynamics by the configuration of a Skyrmion and antiSkyrmion nearing each other. Such a configuration at the point of closest approach is used in Section 3 to obtain a coherent state amplitude describing the pion radiation from annihilation. Interaction between the Skyrmion and antiSkyrmion or among the pions is not considered. In section 4, we discuss the random grooming of the Skyrmion and antiSkyrmion sources and resulting pion correlations. Section 5 outlines the case of Lorentz transformed Skyrmions and compares the results with those from the Galilean case. Section 6 gives our results and prospect for future development. The various approximations we make, some of them quite drastic, are discussed in the sections where they are employed.

II. CLASSICAL MOVING HEDGEHOGS: GALILEAN CASE

The large N_c dynamics we consider is the Skyrme model [9] which is a classical nonlinear field theory of pions only in which the baryons emerge as nonperturbative topological solitons. These baryons are not nucleons but rather hedgehogs (so called because the pion isospin and spatial directions are correlated). The hedgehogs are a superposition of all possible baryonic states with isospin equal to spin. The nucleon, or antinucleon, is then projected out from the hedgehog configuration by grooming or rotating the hedgehog. When a hedgehog and antihedgehog approach each other, there is a complicated interaction coming from the nonlinear nature of the Skyrme dynamics, leading finally to pion radiation. This at least is what happens for close collisions, and has been seen in the one full calculation that has been done. [4] The nonlinear nature of the Skyrme lagrangian and the presence of fourth order derivatives makes the calculation numerically unstable. Thus a full investigation of the nature of Skyrmion antiSkyrmion collisions as a function of energy and impact parameter and of the subsequent pion radiation has not yet been carried out even for the hedgehog anti-hedgehog orientation, let alone for groomed hedgehogs. We do not even try. Rather

3

we take as the initial state a hedgehog and antihedgehog moving in opposite directions and at their point of closest approach. This is the product ansatz for moving hedgehogs. The hedgehogs themselves we take as solutions of the Skyrme equations. We then use their classical pion configuration as the source of pions for our quantum coherent state with no further dynamics among those pions. The calculation of the Cal Tech group [4] and the one model calculation we carried out in simple geometry [10] suggest that once annihilation begins, it proceeds very rapidly, at the causal limit, and that the subsequent pion wave in the radiation zone looks very much like the wave one would obtain from a free wave fourier transform of the source. We use these facts and the fact that anything else is too difficult for now to justify our simple approximations.

In the center of mass, we represent the colliding nucleon and antinucleon by a classical Skyrmion and antiSkyrmion approaching each other with velocity v and impact parameter b.[1] We make the approximation that annihilation and the subsequent pion radiation comes at the instance of closest approach, as shown in Fig. 1. Final state interactions among the resulting pions are neglected as discussed above.

The pion field configuration of a moving hedgehog is the Lorentz boosted static hedgehog. For small velocities, we can approximate it by a Galilei boosted hedgehog, which we study first.

The classical field of pions in Fig. 1 can be written as

$$\vec{\Phi}(\boldsymbol{r}, t) = \vec{\Phi}_a(\boldsymbol{r}, t) + \vec{\Phi}_b(\boldsymbol{r}, t)$$

$$\vec{\Phi}_a(\boldsymbol{r}, t) = (\boldsymbol{r} - \boldsymbol{v}t + \boldsymbol{b}/2)g(|\boldsymbol{r} - \boldsymbol{v}t + \boldsymbol{b}/2|)$$

$$\vec{\Phi}_b(\boldsymbol{r}, t) = -(\boldsymbol{r} + \boldsymbol{v}t - \boldsymbol{b}/2)g(|\boldsymbol{r} + \boldsymbol{v}t - \boldsymbol{b}/2|) \tag{1}$$

where $g(r) = f(r)/r$ ($f(r)$ is the usual Skyrme profile function, modulo f_π), a is the Skyrmion and b is the antiSkyrmion. The fact that the iso-vector fields on the left in (1) are written in terms of radial spatial vectors on the right is the hedgehog feature.

———

[1] Bold face letters denote 3-vectors. Overhead arrows denote iso-vectors.

III. REQUANTIZING

To form a coherent state, we need to decompose the classical pion field (1) into a plane wave and pick out the positive frequency part. We neglect the pion interactions and thus the pion wave satisfies the free wave equation (the isospin index is suppressed for now),

$$\nabla^2 \psi(\boldsymbol{r}, t) = (\frac{\partial^2}{\partial t^2} + m^2)\psi(\boldsymbol{r}, t) \tag{2}$$

where m is the pion mass.

We introduce the momentum space amplitude $h(\boldsymbol{k}, \omega)$ by

$$\psi(\boldsymbol{r}, t) = \int d^3k\, d\omega\, e^{i\boldsymbol{k}\cdot\boldsymbol{r}} e^{-i\omega t} h(\boldsymbol{k}, \omega) \tag{3}$$

and we find

$$h(\boldsymbol{k}, \omega) = \delta(k^2 + m^2 - \omega^2) G(\boldsymbol{k}, \omega) \tag{4}$$

and therefore

$$\psi(\boldsymbol{r}, t) = \int d^3k\, d\omega (e^{i\boldsymbol{k}\cdot\boldsymbol{r}} e^{-i\omega_k t} G(\boldsymbol{k}, \omega_k)/(2\omega_k) + e^{-i\boldsymbol{k}\cdot\boldsymbol{r}} e^{i\omega_k t} G(\boldsymbol{k}, -\omega_k)/(2\omega_k)). \tag{5}$$

The positive frequency part of the wave comes from the first term, the one with $e^{-i\omega_k t}$ and therefore we need $G(\boldsymbol{k}, \omega_k)$, $(\omega_k = \sqrt{k^2 + m^2})$. From the field and its rate of change at $t = 0$, the instant of nearest approach, we obtain

$$\psi(\boldsymbol{r}, 0) = \int d^3k\, e^{i\boldsymbol{k}\cdot\boldsymbol{r}} \frac{G(\boldsymbol{k}, \omega_k) + G(\boldsymbol{k}, -\omega_k)}{2\omega_k}$$
$$= \int d^3k\, e^{i\boldsymbol{k}\cdot\boldsymbol{r}} \gamma_1(\boldsymbol{k}) \tag{6}$$

and

$$\frac{d\psi(\boldsymbol{r}, 0)}{dt} = \int d^3k\, e^{i\boldsymbol{k}\cdot\boldsymbol{r}} (-i) \frac{G(\boldsymbol{k}, \omega_k) - G(\boldsymbol{k}, -\omega_k)}{2}$$
$$= \int d^3k\, e^{i\boldsymbol{k}\cdot\boldsymbol{r}} \gamma_2(\boldsymbol{k}) \tag{7}$$

We therefore see that

5

$$G(\boldsymbol{k}, \omega_k) = \omega_k \gamma_1(\boldsymbol{k}) + i\gamma_2(\boldsymbol{k}) \tag{8}$$

and the fourier amplitude of the field that we need is given by

$$h(\boldsymbol{k}, \omega_k) = \frac{G(\boldsymbol{k}, \omega_k)}{2\omega_k} \tag{9}$$

To obtain γ_1, γ_2 and thus $G(k)$, we fourier transform the field configuration (1) and its time derivative

$$\vec{\gamma}_1(\boldsymbol{k}) = \frac{1}{(2\pi)^3} \int d^3 r e^{-i\boldsymbol{k}\cdot\boldsymbol{r}} \vec{\Phi}(\boldsymbol{r}, 0) \tag{10}$$

$$\vec{\gamma}_2(\boldsymbol{k}) = \frac{1}{(2\pi)^3} \int d^3 r e^{-i\boldsymbol{k}\cdot\boldsymbol{r}} \frac{d\vec{\Phi}}{dt}(\boldsymbol{r}, 0) \tag{11}$$

We split the amplitude into its contributions from the hedgehog and from the antihedgehog.

$$\gamma \to \gamma_a + \gamma_b \tag{12}$$

$$\vec{\gamma}_{1a} = \frac{1}{(2\pi)^3} \int d^3 r e^{-i\boldsymbol{k}\cdot\boldsymbol{r}} (\boldsymbol{r} + \frac{\boldsymbol{b}}{2}) g(|\boldsymbol{r} + \frac{\boldsymbol{b}}{2}|) \tag{13}$$

$$\vec{\gamma}_{1b} = -\frac{1}{(2\pi)^3} \int d^3 r e^{-i\boldsymbol{k}\cdot\boldsymbol{r}} (\boldsymbol{r} - \frac{\boldsymbol{b}}{2}) g(|\boldsymbol{r} - \frac{\boldsymbol{b}}{2}|) \tag{14}$$

Introducing

$$G(k^2) = \frac{1}{(2\pi)^3} \int d^3 \rho e^{-i\boldsymbol{k}\cdot\boldsymbol{\rho}} g(|\boldsymbol{\rho}|) \tag{15}$$

it is easy to show that

$$\vec{\gamma}_{1a} = 2i\boldsymbol{k} e^{i\boldsymbol{k}\cdot\frac{\boldsymbol{b}}{2}} G'(k^2) \tag{16}$$

$$\vec{\gamma}_{1b} = -2i\boldsymbol{k} e^{-i\boldsymbol{k}\cdot\frac{\boldsymbol{b}}{2}} G'(k^2) \tag{17}$$

with $G'(k^2) = dG/d(k^2)$.

$$\dot{\vec{\Phi}}_a(\boldsymbol{r}, 0) = -\boldsymbol{v} g(|\boldsymbol{r} + \frac{\boldsymbol{b}}{2}|^2) - (\boldsymbol{r} + \frac{\boldsymbol{b}}{2}) \boldsymbol{v} \cdot 2(\boldsymbol{r} + \frac{\boldsymbol{b}}{2}) g'(|\boldsymbol{r} + \frac{\boldsymbol{b}}{2}|^2) \tag{18}$$

$$\dot{\vec{\Phi}}_b(\boldsymbol{r}, 0) = -\boldsymbol{v} g(|\boldsymbol{r} - \frac{\boldsymbol{b}}{2}|^2) - (\boldsymbol{r} - \frac{\boldsymbol{b}}{2}) \boldsymbol{v} \cdot 2(\boldsymbol{r} - \frac{\boldsymbol{b}}{2}) g'(|\boldsymbol{r} - \frac{\boldsymbol{b}}{2}|^2) \tag{19}$$

6

where

$$g'(\boldsymbol{\rho}^2) = \frac{dg}{d\boldsymbol{\rho}^2} \tag{20}$$

It is straightforward to show

$$\vec{\gamma}_{2a} = \frac{1}{(2\pi)^3} \int d^3r e^{-i\boldsymbol{k}\cdot\boldsymbol{r}} \dot{\vec{\Phi}}_a(\boldsymbol{r}, 0)$$

$$= -\boldsymbol{v}e^{i\boldsymbol{k}\cdot\frac{\boldsymbol{b}}{2}}G(k^2) + \vec{\gamma}_{2a}^{II} \tag{21}$$

where

$$\vec{\gamma}_{2a}^{II} = \frac{1}{(2\pi)^3} \int d^3r e^{-i\boldsymbol{k}\cdot\boldsymbol{r}}(\boldsymbol{r} + \frac{\boldsymbol{b}}{2})[-2\boldsymbol{v}\cdot(\boldsymbol{r} + \frac{\boldsymbol{b}}{2})]g'(|\boldsymbol{r} + \frac{\boldsymbol{b}}{2}|)$$

$$= \frac{1}{(2\pi)^3}e^{i\boldsymbol{k}\cdot\frac{\boldsymbol{b}}{2}} \int d^3\rho e^{-i\boldsymbol{k}\cdot\boldsymbol{\rho}}\boldsymbol{\rho}(-2\boldsymbol{v}\cdot\boldsymbol{\rho})g'(\rho^2)$$

$$= -\frac{1}{(2\pi)^3}e^{i\boldsymbol{k}\cdot\frac{\boldsymbol{b}}{2}} \int d^3\rho e^{-i\boldsymbol{k}\cdot\boldsymbol{\rho}}\boldsymbol{v}\cdot\boldsymbol{\rho}\nabla_\rho g(\rho^2)$$

$$= \frac{1}{(2\pi)^3}e^{i\boldsymbol{k}\cdot\frac{\boldsymbol{b}}{2}} \int d^3\rho g(\rho^2)\nabla_\rho[e^{-i\boldsymbol{k}\cdot\boldsymbol{\rho}}\boldsymbol{v}\cdot\boldsymbol{\rho}]$$

$$= e^{i\boldsymbol{k}\cdot\frac{\boldsymbol{b}}{2}}\boldsymbol{v}G(k^2) + 2e^{i\boldsymbol{k}\cdot\frac{\boldsymbol{b}}{2}}\boldsymbol{k}\,\boldsymbol{v}\cdot\boldsymbol{k}G'(k^2) \tag{22}$$

Note we use $\nabla_\rho g(\rho^2) = 2\boldsymbol{\rho}\frac{dg}{d\rho^2}$ and then integrate by parts. Thus the fourier amplitude (9) of the field of the Skyrmion we need is

$$\vec{h}_a(\boldsymbol{k}, \omega_k) = i\boldsymbol{k}e^{i\boldsymbol{k}\cdot\frac{\boldsymbol{b}}{2}}G'(k^2)(1 + \frac{\boldsymbol{v}\cdot\boldsymbol{k}}{\omega_k}) \tag{23}$$

Similarly we have for the field from the antiSkyrmion

$$\vec{h}_b(\boldsymbol{k}, \omega_k) = -i\boldsymbol{k}e^{-i\boldsymbol{k}\cdot\frac{\boldsymbol{b}}{2}}G'(k^2)(1 - \frac{\boldsymbol{v}\cdot\boldsymbol{k}}{\omega_k}) \tag{24}$$

A quantum coherent state represent the configuration in Fig. 1 can then be written as

$$|h\rangle = \exp[\int d^3k(\vec{h}_a(\boldsymbol{k}, \omega_k) + \vec{h}_b(\boldsymbol{k}, \omega_k))\cdot\vec{a}^+(\boldsymbol{k})]|0\rangle \tag{25}$$

IV. RANDOM GROOMING AND CORRELATIONS

We next consider grooming of the hedgehog and anti-hedgehog to introduce spin and isospin. In fact we will argue that we do not have to quantize the grooming but that we can consider random grooming. This is justified by consideration of time scales. Spin and isospin are introduced by spinning or rotating the hedgehog at a fixed rate. That rate of rotation is slow compared to the annihilation time. Thus during any given annihilation the groomed hedgehogs do not rotate much. But if there is no polarization, their orientation is random at the moment of annihilation and it is that random orientation or random grooming that we average over when we consider many events.

As shown in the calculation of Skyrmion and antiSkyrmion annihilation [4,10], the pions emerge promptly from the interaction region. This happens in about the time for light signal to travel across the Skyrmion, which is $T_c = 1/m$. Here m is the pion mass. The rotation period can be estimated from the $N - \Delta$ splitting which is of the order of m. The rotation energy is $E_r \approx Ir^2\omega^2 \approx M/(m^2T_r^2) \sim m$, thus $T_r = 1/m\sqrt{M/m}$. M is the nucleon mass. The ratio of rotation to annihilation time is then $T_r/T_c \sim \sqrt{M/m} \approx 3$. If we were to estimate the rotation time by the angular momentum (of order 1, noting $\hbar = 1$), we would have $J \sim I\omega \sim M/m^2/T_r \sim 1$ and $T_r = M/m^2$. The ratio would be $T_r/T_c \sim M/m \approx 7$. Both these estimates suggest that the approximation of taking a fixed orientation during the fast annihilation is a reasonable one. This is something that should be improved in more detailed calculations. In the limit of slow rotation, the isospin orientation of each Skyrmion can be considered as random between one annihilation event and another. Experimental observables should then be the average over all the different directions in isospin space.

To proceed with random grooming, we write the amplitudes $h(\boldsymbol{k})$ in spherical components

$$h_{a\mu} = \sqrt{\frac{4\pi}{3}} Y_{1\mu}(\hat{k}) H_a(\boldsymbol{k})$$

$$h_{b\mu} = \sqrt{\frac{4\pi}{3}} Y_{1\mu}(\hat{k}) H_b(\boldsymbol{k}) \tag{26}$$

with

$$H_a(\boldsymbol{k}) = ie^{i\boldsymbol{k}\cdot\frac{\boldsymbol{b}}{2}}kG'(k^2)(1 + \frac{\boldsymbol{v}\cdot\boldsymbol{k}}{\omega_k})$$

$$H_b(\boldsymbol{k}) = -ie^{-i\boldsymbol{k}\cdot\frac{\boldsymbol{b}}{2}}kG'(k^2)(1 - \frac{\boldsymbol{v}\cdot\boldsymbol{k}}{\omega_k}) \tag{27}$$

Independent grooming of the Skyrmion and anti-Skyrmion means identifying the total amplitude with the μ-th component of isospin as

$$h_\mu(\boldsymbol{k},\Omega,\Xi) = \sqrt{\frac{4\pi}{3}} \left[\mathcal{D}^1_{\mu\nu}(\Omega)Y_{1\nu}(\hat{k})H_a(\boldsymbol{k}) + \mathcal{D}^1_{\mu\nu}(\Xi)Y_{1\nu}(\hat{k})H_b(\boldsymbol{k}) \right] \tag{28}$$

with Ω and Ξ being two sets of independent Euler angles. Observables calculated from the coherent state (25) with the amplitude (28) are to be averaged over the range of Ω and Ξ.

First we examine the one-body rate, that is the probability for finding a pion of momentum $\boldsymbol{k}$ and isospin type μ in the coherent state. We have

$$
\begin{aligned}
W^{(1)}(\mu,\boldsymbol{k}) = {} & \frac{1}{(8\pi^2)^2} \int d\Omega d\Xi \, h^*_\mu(\boldsymbol{k},\Omega,\Xi) \, h_\mu(\boldsymbol{k},\Omega,\Xi) \\
= {} & \frac{1}{48\pi^3} \int d\Omega d\Xi \\
& \left[\mathcal{D}^{1*}_{\mu\nu}(\Omega)\mathcal{D}^1_{\mu\nu'}(\Omega)H^*_a(\boldsymbol{k})H_a(\boldsymbol{k}) \right. \\
& + \mathcal{D}^{1*}_{\mu\nu}(\Xi)\mathcal{D}^1_{\mu\nu'}(\Xi)H^*_b(\boldsymbol{k})H_b(\boldsymbol{k}) \\
& + \mathcal{D}^{1*}_{\mu\nu}(\Omega)\mathcal{D}^1_{\mu\nu'}(\Xi)H^*_a(\boldsymbol{k})H_b(\boldsymbol{k}) \\
& \left. + \mathcal{D}^{1*}_{\mu\nu}(\Xi)\mathcal{D}^1_{\mu\nu'}(\Omega)H^*_b(\boldsymbol{k})H_a(\boldsymbol{k}) \right] Y^*_{1\nu}(\hat{k})Y_{1\nu'}(\hat{k})
\end{aligned}
\tag{29}
$$

After the angular average, we obtain

$$
\begin{aligned}
W^{(1)}(\mu,\boldsymbol{k}) = {} & \frac{1}{3} \left[H^*_a(\boldsymbol{k})H_a(\boldsymbol{k}) + H^*_b(\boldsymbol{k})H_b(\boldsymbol{k}) \right] \\
= {} & \frac{1}{3}k^2(G'(k^2))^2 \left[(1 + \frac{\boldsymbol{v}\cdot\boldsymbol{k}}{\omega_k})^2 + (1 - \frac{\boldsymbol{v}\cdot\boldsymbol{k}}{\omega_k})^2 \right]
\end{aligned}
\tag{30}
$$

which is independent of μ and the impact parameter $\boldsymbol{b}$, as we expect of a one-body observable averaged over independent groomings.

Next we look at the 2-body rate, that is the probability of finding a pion of momentum $\boldsymbol{k}$ and charge type μ and a pion of momentum $\boldsymbol{q}$ and charge type ρ in the state $|h\rangle$. We have

$$W^{(2)}(\mu, \boldsymbol{k}; \rho, \boldsymbol{q}) = \frac{1}{(8\pi^2)^2} \int d\Omega d\Xi \, h_\mu^*(\boldsymbol{k}, \Omega, \Xi) \, h_\mu(\boldsymbol{k}, \Omega, \Xi) \, h_\rho^*(\boldsymbol{q}, \Omega, \Xi) \, h_\rho(\boldsymbol{q}, \Omega, \Xi)$$

$$= \frac{1}{36\pi^2} \int d\Omega d\Xi$$

$$\left[\mathcal{D}_{\mu\nu}^{1*}(\Omega) \mathcal{D}_{\mu\nu'}^{1}(\Omega) \mathcal{D}_{\rho\sigma}^{1*}(\Omega) \mathcal{D}_{\rho\sigma'}^{1}(\Omega) H_a^*(\boldsymbol{k}) H_a(\boldsymbol{k}) H_a^*(\boldsymbol{q}) H_a(\boldsymbol{q}) \right.$$

$$+ \mathcal{D}_{\mu\nu}^{1*}(\Omega) \mathcal{D}_{\mu\nu'}^{1}(\Omega) \mathcal{D}_{\rho\sigma}^{1*}(\Omega) \mathcal{D}_{\rho\sigma'}^{1}(\Xi) H_a^*(\boldsymbol{k}) H_a(\boldsymbol{k}) H_a^*(\boldsymbol{q}) H_b(\boldsymbol{q})$$

$$+ \mathcal{D}_{\mu\nu}^{1*}(\Omega) \mathcal{D}_{\mu\nu'}^{1}(\Omega) \mathcal{D}_{\rho\sigma}^{1*}(\Xi) \mathcal{D}_{\rho\sigma'}^{1}(\Omega) H_a^*(\boldsymbol{k}) H_a(\boldsymbol{k}) H_b^*(\boldsymbol{q}) H_a(\boldsymbol{q})$$

$$+ \mathcal{D}_{\mu\nu}^{1*}(\Omega) \mathcal{D}_{\mu\nu'}^{1}(\Omega) \mathcal{D}_{\rho\sigma}^{1*}(\Xi) \mathcal{D}_{\rho\sigma'}^{1}(\Xi) H_a^*(\boldsymbol{k}) H_a(\boldsymbol{k}) H_b^*(\boldsymbol{q}) H_b(\boldsymbol{q})$$

$$+ \mathcal{D}_{\mu\nu}^{1*}(\Omega) \mathcal{D}_{\mu\nu'}^{1}(\Xi) \mathcal{D}_{\rho\sigma}^{1*}(\Omega) \mathcal{D}_{\rho\sigma'}^{1}(\Omega) H_a^*(\boldsymbol{k}) H_b(\boldsymbol{k}) H_a^*(\boldsymbol{q}) H_a(\boldsymbol{q})$$

$$+ \mathcal{D}_{\mu\nu}^{1*}(\Omega) \mathcal{D}_{\mu\nu'}^{1}(\Xi) \mathcal{D}_{\rho\sigma}^{1*}(\Omega) \mathcal{D}_{\rho\sigma'}^{1}(\Xi) H_a^*(\boldsymbol{k}) H_b(\boldsymbol{k}) H_a^*(\boldsymbol{q}) H_b(\boldsymbol{q})$$

$$+ \mathcal{D}_{\mu\nu}^{1*}(\Omega) \mathcal{D}_{\mu\nu'}^{1}(\Xi) \mathcal{D}_{\rho\sigma}^{1*}(\Xi) \mathcal{D}_{\rho\sigma'}^{1}(\Omega) H_a^*(\boldsymbol{k}) H_b(\boldsymbol{k}) H_b^*(\boldsymbol{q}) H_a(\boldsymbol{q})$$

$$+ \mathcal{D}_{\mu\nu}^{1*}(\Omega) \mathcal{D}_{\mu\nu'}^{1}(\Xi) \mathcal{D}_{\rho\sigma}^{1*}(\Xi) \mathcal{D}_{\rho\sigma'}^{1}(\Xi) H_a^*(\boldsymbol{k}) H_b(\boldsymbol{k}) H_b^*(\boldsymbol{q}) H_b(\boldsymbol{q})$$

$$\left. + (a \leftrightarrow b, \Omega \leftrightarrow \Xi) \right] Y_{1\nu}^*(\hat{k}) Y_{1\nu'}(\hat{k}) Y_{1\sigma}^*(\hat{q}) Y_{1\sigma'}(\hat{q}) \tag{31}$$

Terms with odd numbers of Ω or Ξ average to zero. Applying the following formulae for Wigner functions

$$\int \mathcal{D}_{\mu\nu}^{1*} \mathcal{D}_{\rho\sigma}^{1} = \frac{8\pi^2}{3} \delta_{\mu\rho} \delta_{\nu\sigma}, \tag{32}$$

$$\int \mathcal{D}_{\mu\nu}^{1} \mathcal{D}_{\rho\sigma}^{1} = (-1)^{\mu-\nu} \int \mathcal{D}_{-\mu-\nu}^{1*} \mathcal{D}_{\rho\sigma}^{1}$$

$$= \frac{8\pi^2}{3} (-1)^{\mu-\nu} \delta_{\mu,-\rho} \delta_{\nu,-\sigma}, \tag{33}$$

$$\int \mathcal{D}_{\mu\nu}^{1*} \mathcal{D}_{\rho\sigma}^{1*} \mathcal{D}_{\mu\nu'}^{1} \mathcal{D}_{\rho\sigma'}^{1} = 8\pi^2 \sum_{\Lambda M M'} \frac{1}{2\Lambda+1} \langle 11; \mu\rho | \Lambda M \rangle^2 \langle 11; \nu\sigma | \Lambda M' \rangle \langle 11; \nu'\sigma' | \Lambda M' \rangle, \tag{34}$$

the two-body rate is then

$$W^{(2)}(\mu, \boldsymbol{k}; \rho, \boldsymbol{q}) = \frac{1}{9} \left[A_{\mu\rho}(z)(H_a^*(\boldsymbol{k}) H_a(\boldsymbol{k}) H_a^*(\boldsymbol{q}) H_a(\boldsymbol{q}) + (a \leftrightarrow b)) \right.$$

$$+ B_{\mu\rho}(z)(H_a^*(\boldsymbol{k}) H_a(\boldsymbol{k}) H_b^*(\boldsymbol{q}) H_b(\boldsymbol{q}) + (a \leftrightarrow b))$$

$$+ C_{\mu\rho}(z)(H_a^*(\boldsymbol{k}) H_b(\boldsymbol{k}) H_a^*(\boldsymbol{q}) H_b(\boldsymbol{q}) + (a \leftrightarrow b))$$

$$\left. + D_{\mu\rho}(z)(H_a^*(\boldsymbol{k}) H_b(\boldsymbol{k}) H_b^*(\boldsymbol{q}) H_a(\boldsymbol{q}) + (a \leftrightarrow b)) \right] \tag{35}$$

10

where

$$A_{\mu\rho}(z) = 9 \sum_{L\Lambda} (-1)^L \langle 11; \mu\rho|LM \rangle^2 \langle 11; 00|\Lambda 0 \rangle^2 W(1111; L\Lambda) P_\Lambda(z) \tag{36}$$

$$B_{\mu\rho}(z) = 1 \tag{37}$$

$$C_{\mu\rho}(z) = \delta_{\mu,-\rho} z^2 \tag{38}$$

$$D_{\mu\rho}(z) = \delta_{\mu,\rho} z^2 \tag{39}$$

with $z = \hat{k} \cdot \hat{q}$.

Putting the explicit forms of H_a and H_b (27) into $W^{(2)}$, we have

$$
\begin{aligned}
W^{(2)} = \; & \tfrac{1}{9} \, k^2 (G'(k^2))^2 q^2 (G'(q^2))^2 \big[\\
& A_{\mu\rho}(z) \left((1 + \frac{\boldsymbol{v} \cdot \boldsymbol{k}}{\omega_k})^2 (1 + \frac{\boldsymbol{v} \cdot \boldsymbol{q}}{\omega_q})^2 + (1 - \frac{\boldsymbol{v} \cdot \boldsymbol{k}}{\omega_k})^2 (1 - \frac{\boldsymbol{v} \cdot \boldsymbol{q}}{\omega_q})^2 \right) \\
& + \left((1 + \frac{\boldsymbol{v} \cdot \boldsymbol{k}}{\omega_k})^2 (1 - \frac{\boldsymbol{v} \cdot \boldsymbol{q}}{\omega_q})^2 + (1 + \frac{\boldsymbol{v} \cdot \boldsymbol{q}}{\omega_q})^2 (1 - \frac{\boldsymbol{v} \cdot \boldsymbol{k}}{\omega_k})^2 \right) \\
& + \delta_{\mu,-\rho} z^2 \left(1 - (\frac{\boldsymbol{v} \cdot \boldsymbol{k}}{\omega_k})^2 \right) \left(1 - (\frac{\boldsymbol{v} \cdot \boldsymbol{q}}{\omega_q})^2 \right) 2 \cos((\boldsymbol{k} + \boldsymbol{q}) \cdot \boldsymbol{b}) \\
& + \delta_{\mu\rho} z^2 \left(1 - (\frac{\boldsymbol{v} \cdot \boldsymbol{k}}{\omega_k})^2 \right) \left(1 - (\frac{\boldsymbol{v} \cdot \boldsymbol{q}}{\omega_q})^2 \right) 2 \cos((\boldsymbol{k} - \boldsymbol{q}) \cdot \boldsymbol{b}) \big]
\end{aligned}
\tag{40}
$$

The quantity $A_{\mu\rho}(z)$ (36) is easily evaluated to be

$$
A_{\mu\rho}(z) = \begin{cases}
\frac{9}{10} + \frac{3}{10} z^2 & \text{if } \mu \neq 0 \text{ and } \rho \neq 0 \\
\frac{6}{5} - \frac{3}{5} z^2 & \text{if only } \mu \text{ or } \rho \text{ is zero} \\
\frac{3}{5} + \frac{6}{5} z^2 & \text{if } \mu = 0 \text{ and } \rho = 0
\end{cases}
\tag{41}
$$

We should also observe that

$$A_{\mu\rho}(z) = A_{\rho\mu}(z), \quad \sum_{\mu\rho} A_{\mu\rho}(z) = 9. \tag{42}$$

There are two kinds of pion correlations studied in the literature. The first is the standard correlation function defined by

$$C_2(\mu, \boldsymbol{p}; \rho, \boldsymbol{q}) = \frac{W_2(\mu, \boldsymbol{p}; \rho, \boldsymbol{q})}{W_1(\mu, \boldsymbol{p}) W_1(\rho, \boldsymbol{q})} - 1 \tag{43}$$

and the second form, most used in extracting pion correlations from annihilation data, is

$$R_2(\mu, \boldsymbol{p}; \nu, \boldsymbol{q})/(\rho, \boldsymbol{p}; \sigma, \boldsymbol{q}) = \frac{W_2(\mu, \boldsymbol{p}; \nu, \boldsymbol{q})}{W_2(\rho, \boldsymbol{p}; \sigma, \boldsymbol{q})}. \tag{44}$$

This form is suitable for studying correlations from many random sources, where the two-body rates for different type of particles (like $\pi^+\pi^-$) approaches the product of the corresponding one-body rates. This form is commonly used for ratios of correlations among like to unlike pions (eg $\mu = \nu$).

Annihilation occurs over a range of the impact parameter $\boldsymbol{b}$. Substantial annihilation is expected for $b \leq 1\mathrm{fm}$ while it should be minimal for b much large than 1fm. To further examine the correlations, we average over the impact parameter $\boldsymbol{b}$ with the probability $e^{-\lambda b}$. Here λ is a range parameter of the order of one inverse fermi, specifying the significant region of collision of Skyrmion and anti-Skyrmion. In the two-body rate (40) only the last two terms depend on $\boldsymbol{b}$. The integral needed for the average is

$$\int d^2 b\, e^{-\lambda b} \cos(\boldsymbol{Q} \cdot \boldsymbol{b}) = \int db\, d\phi\, b\, e^{-\lambda b} \cos(Q_\perp b \cos \phi) \tag{45}$$

where $\boldsymbol{Q} = \boldsymbol{k} \pm \boldsymbol{q}$, $Q_\perp$ is the magnitude of the component of $\boldsymbol{Q}$ in the $\boldsymbol{b}$ plane, and ϕ is the angle between this component and $\boldsymbol{b}$. This integral gives

$$\frac{2\pi\lambda}{(\lambda^2 + Q_\perp^2)^{\frac{3}{2}}}. \tag{46}$$

The result of such an averaging is achieved simply by replacing $\cos(\boldsymbol{Q} \cdot \boldsymbol{b})$ by $\lambda^3/(\lambda^2 + Q_\perp^2)^{\frac{3}{2}}$ in (40).

V. LORENTZ TRANSFORMED HEDGEHOG

When the velocity of the moving hedgehog is not small compared to the speed of light, the Lorentz transformed field configuration should be used. In the overall CM frame, the moving hedgehog (in the direction of positive x-axis) $\vec{\phi}_a$ in (1) can be written as

$$\vec{\phi}_a = (\gamma(x - vt), y + b/2, z)\gamma^2 g((x - vt)^2 + (y + b/2)^2 + z^2) \tag{47}$$

considering that the pion field transforms as a pseudo-scalar. Here $\gamma = 1/\sqrt{1 - v^2/c^2}$. Similarly the Lorentz transformed anti-Skyrmion is

12

$$\vec{\phi_b} = -(\gamma(x + vt), y - b/2, z)g(\gamma^2(x + vt)^2 + (y - b/2)^2 + z^2) \tag{48}$$

Compare (47), (48) with the Galilean boosted field configurations 1 and their Fourier transforms 10, we define the following "capitalized" quantities

$$\boldsymbol{V} = \gamma\boldsymbol{v}$$

$$\boldsymbol{R} = (\gamma x, y, z)$$

$$\boldsymbol{K} = (k_x/\gamma, k_y, k_z). \tag{49}$$

The calculation of the fourier amplitudes for the Lorentz case is essentially the same as in the Galilean case, if we replace the lower case vectors in the Galilean case by these "capitalized" vectors. We should also note that $d^3r = \frac{1}{\gamma}d^3R$.

The Fourier amplitudes for the Skyrmion and antiSkyrmion are then

$$\frac{1}{\gamma}\vec{h}_a(\boldsymbol{K}, \omega_k) = i\frac{\boldsymbol{K}}{\gamma}e^{i\boldsymbol{k}\cdot\frac{\boldsymbol{b}}{2}}G'(K^2)(1 + \frac{\mathbf{v}\cdot\mathbf{k}}{\omega_k}) \tag{50}$$

$$\frac{1}{\gamma}\vec{h}_a(\boldsymbol{K}, \omega_k) = -i\frac{\boldsymbol{K}}{\gamma}e^{i\boldsymbol{k}\cdot\frac{\boldsymbol{b}}{2}}G'(K^2)(1 - \frac{\mathbf{v}\cdot\mathbf{k}}{\omega_k}) \tag{51}$$

Independent random grooming on the (anti)hedgehog is simply a rotation on the vector $\boldsymbol{K}$ for the Lorentz case. Consequently, the one-body and two body rates, (30) and (35), are replaced by

$$W_L^{(1)}(\mu, \boldsymbol{k}) = \frac{1}{\gamma^2}W_G^{(1)}(\mu, \boldsymbol{K}) \tag{52}$$

and

$$W_L^{(2)}(\mu, \boldsymbol{k}; \nu, \boldsymbol{q}) = \frac{1}{\gamma^4}W_G^{(2)}(\mu, \boldsymbol{K}; \nu, \boldsymbol{Q}) \tag{53}$$

Here L stands for Lorentz and G Galilean. The cosine of the relative angle in (35) should be replaced by $\hat{K}\cdot\hat{Q}$. In the plane perpendicular to the velocity, the two cases give identical pion correlations.

13

VI. RESULT AND DISCUSSION

Pion correlations arise from the incoherence in emission sources, commonly from thermal or experimental averages. In the present case, however, the Skyrme dynamics (in particular, the coupling between spatial and isospin degrees of freedom) also leads to interesting correlations. Although related to the regular type of correlations [5], the present study points to correlations not only among pions of like charges but among unlike charges as well. Our present consideration does not include full dynamical evolution nor final state interactions among the pions. However, we hope important aspects of the Skyrme physics in $N\overline{N}$ annihilation are elucidated here and the qualitative features will remain in a more thorough study.

As an example of what our picture gives for correlations, we study the R_2 of (44). This is the correlation function most commonly studied in annihilation. What is usually studied is not the full R_2 as a function of both momentum variables, but rather R_2 as a function of pion pair relative momentum summed over all total momenta. That is we define $\boldsymbol{Q} = \boldsymbol{p} - \boldsymbol{q}$ and $\boldsymbol{P} = \boldsymbol{p} + \boldsymbol{q}$. Then consider R_2 for fixed Q summed over all $\boldsymbol{P}$ as well as being averaged over the random groomings and impact parameter. Note that after those averages, R_2 is a function of the magnitude of Q only. We study R_2 using the Lorentz boosted form for two values of the incident energy, or velocity, $v = 0.1c$ and $v = 0.9c$. In the sum over $\boldsymbol{P}$ for fixed $\boldsymbol{Q}$ we take into account the constraints of energy and momentum conservation. In order to do this calculation we need to choose a form for $G(k^2)$ defined in (15). We take the simple form, $G(k^2) = 1/(k^2 + \mu^2)$, and take $\mu = \lambda = 1\text{fm}^{-1}$, where λ is the range in the impact parameter average. We study R_2 as a function of Q for various charge ratios. These are shown in Figure 2. For all cases R_2 tends to one for large Q, reflecting the absence of charge correlations for large relative momentum. The range over which R_2 differs significantly from one is 1fm^{-1} and is set by our choice of scale. In all cases the like charge pion to unlike charge correlations resemble closely the correlations seen in the data and usually attributed to Bose-Einstein effects. Note that we see them here although we have made no statistical

or thermal assumptions. As we have discussed before [5], we have averaged over $\boldsymbol{P}$, impact parameter and grooming.

Similar correlations (especially among unlike charged pions) has been discussed [8] for heavy ion collisions as a consequence of Skyrme dynamics. However, it may be easier to examine these correlations experimentally in $N\overline{N}$ annihilation since the dynamics is much simpler. In further extending our study of the manifestation of large QCD in annihilation, we need to study quantum corrections, time dependent rotational Skyrmions and their collisions, interactions among the emitted pion waves and the construction of a coherent state representing a half integer spin soliton. These considerations may hold the clue to two-pion charge-spin asymmetry [6] and other interesting experimental findings [11]. These studies will extend the domain of the classical/quantum approach to annihilation physics.

15

REFERENCES

[1] R.D. Amado, F. Cannata, J-P. Dedonder, M.P. Locher, and B. Shao, Phys. Rev. Lett. **72**, 970 (1994); Phys. Rev. **C 50**, 640 (1994).

[2] B. Shao and R.D. Amado, Phys. Rev. **C 50**, 1787 (1994).

[3] Yang Lu and R.D. Amado, hep-ph/9504362 and nucl-th/9505021.

[4] H.M. Sommermann, R. Seki, S. Larson and S.E. Koonin, Phys. Rev. **D 45**, 4303 (1992).

[5] R. D. Amado, F. Cannata, J.-P. Dedonder, M. P. Locher and Yang Lu, Phys. Lett. **B 339**, 201 (1994); Phys. Rev. **C 51**, 1587 (1995).

[6] A. Hasan et al., Nucl. Phys. **B 378**, 3 (1992).

[7] S. Takeuchi, F. Myhrer and K. Kubodera, Nucl. Phys. **A** 556, 601 (1993).

[8] J.-P. Blaizot and D. Diakonov, Phys. Lett. **B 315**, 226 (1993).

[9] T.H.R. Skyrme, Proc. R. Soc. London **262**, 237 (1961); Nucl. Phys. **31**, 556 (1962).

[10] B. Shao, N.R. Walet and R.D. Amado, Phys. Lett. **B 303**, 1 (1993).

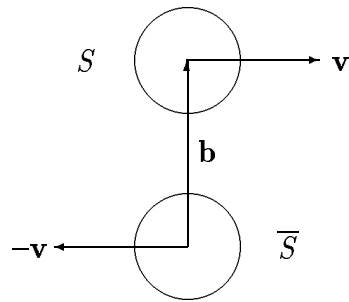[11] C. Amsler and F. Myhrer, Annu. Rev. Nucl. Part. Sci. **41**, 219 (1991).

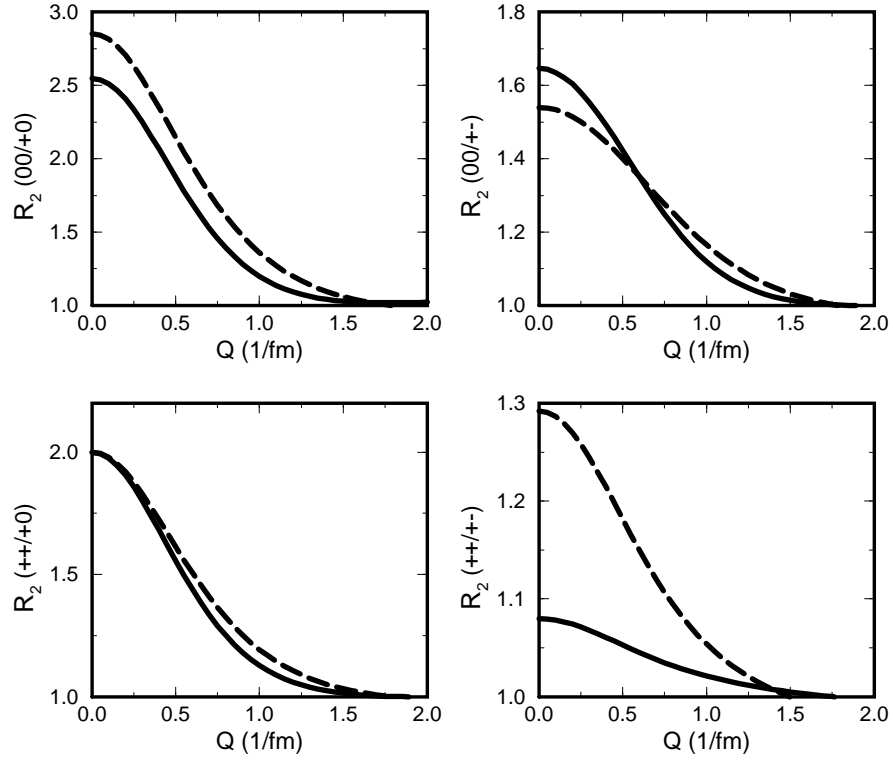FIG. 1. Skyrmion and antiSkyrmion in collision.

FIG. 2. The two pion correlation, R_2 as defined in (44), as a function of pion relative momentum Q after grooming and averaging over total momentum of the two pions and the direction of antiproton velocity (as discussed in the main text). We show here R_2 for different charge combinations. Solid curves are for $v = 0.1c$ and dashed for $v = 0.9c$.